CSMA 2026
17ème Colloque National en Calcul des Structures
18-22 Mai 2026, Presqu'île de Giens (Var)

Structure-preserving discretization of intrinsic geometrically exact beams for explicit multibody dynamics

A. Brugnoli[1], P. L. Kinon[2], F. Sanfedino[3], P. Betsch[2]

[1] *ICA, Université de Toulouse, ISAE-SUPAERO, MINES ALBI, UPS, INSA, CNRS, Toulouse, France*
[2] *Institute of Mechanics, Karlsruhe Institute of Technology (KIT), Otto-Ammann-Platz 9, 76131 Karlsruhe, Germany*
[3] *Féderation ONERA ISAE ENAC, 10 Avenue Marc Pélegrin, Cedex 4, Toulouse, BP-54032, 31055, France*

Résumé — A key challenge in flexible multibody dynamics is the presence of stiff differential–algebraic equations due to kinematic constraints. The Reissner–Simo and Hodges models are two equivalent representations of the dynamics of finite strain beams : the former comes typically as a displacement-based formulation, whereas the latter is intrinsic, meaning that displacement and rotations are not explicitly required. At the numerical level this equivalence is generally lost and each representation offers distinct advantages. In particular, the intrinsic formulation employs linear differential operators, which allow kinematic and dynamic boundary conditions to be imposed naturally through mixed finite elements. In this work, we present a structure-preserving discretization of the intrinsic formulation for assembling multibody systems without algebraic constraints. Through a simple numerical example of closed-loop kinematic chain, we demonstrate that the presented formulation allow to assemble systems without Lagrange multipliers, while energy and momentum are preserved using the implicit midpoint scheme.
Mots clés — Geometrically exact beams, intrinsic formulation, port-Hamiltonian systems, multibody dynamics, structure-preserving discretization, mixed finite elements.

1 Introduction

Flexible rod-like structures appear in many mechanical engineering applications. A widely used modeling approach is the shear-deformable Simo-Reissner formulation [1, 2], which accommodates large rotations and deformations while treating cross sections as rigid. It is well established that this beam model also admits an intrinsic representation, where the dynamics can be expressed without explicitly tracking positions or rotations [3]. See [4] for a formal proof of the equivalence between the intrinsic and displacement-based formulation. The intrinsic form naturally reveals a port-Hamiltonian (pH) structure [5, 6], which can be exploited for state-of-the art simulation and control methodologies. More recently, a pH formulation that equips the displacement-based approach with independent strain measures has been proposed [7]. This framework further avoids shear locking and employs a simple midpoint time integration scheme that guarantees exact energy and momentum preservation. Although the intrinsic formulation offers advantages—such as avoiding rotational parameterizations—its numerical treatment has received comparatively limited attention in the existing literature, see exception [8].

A recurring challenge in flexible multibody dynamics is the presence of stiff differential– algebraic equations arising from kinematic constraints between interconnected components [9]. In displacement-based formulations, such algebraic constraints are unavoidable because the associated finite element framework does not allow a weak enforcement of the kinematic (i.e. Dirichlet) boundary conditions. This limitation stems from the nonlinear appearance of the differential operators. In contrast, the intrinsic formulation features differential operators that enter the equations linearly, allowing kinematic or dynamic boundary conditions to be applied naturally through an appropriate mixed finite element discretization.

In this work, we demonstrate how the pH intrinsic beam formulation can be discretized in

a structure-preserving manner to obtain interconnected multibody systems without algebraic constraints. To this end, we introduce various mixed finite element discretizations that naturally accommodate different boundary conditions. A key feature common to all these discretizations is the satisfaction of compatibility conditions between the finite element spaces, which eliminates shear-locking effects and ensures exact preservation of certain conservation laws in the linear case. While we mostly restrict ourselves to the planar case, the methodology can easily be extended to spatial problems. Energy and momentum are preserved through the implicit midpoint scheme, exploiting the quadratic nature of the energy in the state variables. Additionally, we show that closed-loop kinematic chains can be assembled without the introduction of Lagrange multipliers.

2 Background

Consider a one-dimensional material beam configuration $\Omega = [0, L]$ where L is the beam length. The planar motion of each material point of the centerline is described via the position vector $\boldsymbol{r}(s,t) \in \Omega_t \subset \mathbb{R}^2$, where Ω_t is the spatial configuration at time t. The geometrically exact description of the kinematics is employed by means of an angle $\theta : \Omega \times [0,T] \to \mathbb{R}$, where T is the final time, which parametrizes the rotation matrix :

$$\boldsymbol{\Lambda} = \begin{pmatrix} \cos\theta(s,t) & -\sin\theta(s,t) \\ \sin\theta(s,t) & \cos\theta(s,t) \end{pmatrix},$$

This rotation matrix converts spatial quantities to material quantities. Denoting the material axial stress resultant vector $\boldsymbol{N}$ and the bending moment M, the dynamics take the form :

$$\begin{aligned} \rho A \partial_t^2 \boldsymbol{r} &= \partial_s(\boldsymbol{\Lambda N}) + \boldsymbol{n}_{\text{ext}}, \\ \rho I \partial_t^2 \theta &= \partial_s M + \partial_s \boldsymbol{r}^\top \boldsymbol{S}(\boldsymbol{\Lambda N}) + m_{\text{ext}}, \end{aligned} \tag{1}$$

where ρ is the density, I the second moment of inertia of the cross-section, A the cross-section area, and $\boldsymbol{n}_{\text{ext}}$ and m_{ext} the external spatial distributed forces and moments, respectively. The matrix $\boldsymbol{S}$ formalizes the cross-product in $\mathbb{R}^2$ meaning that :

$$\boldsymbol{v} \times \boldsymbol{u} = \boldsymbol{v}^\top \boldsymbol{S} \boldsymbol{u}, \qquad \boldsymbol{S} := \begin{bmatrix} 0 & 1 \\ -1 & 0 \end{bmatrix}, \qquad \text{for all } \boldsymbol{v}, \boldsymbol{u} \in \mathbb{R}^2.$$

This formulation is equivalent to the intrinsic formulation proposed in [3]. For a formal proof of the equivalence between the two formulations we refer to [4]. Given the spatial velocity $\boldsymbol{v} := \partial_t \boldsymbol{r}$, the material velocity $\boldsymbol{V}$ is given by $\boldsymbol{v} := \boldsymbol{\Lambda V}$. As the motion is planar the spatial ω and material W angular velocities coincide $\partial_t \theta = \omega = W$. Assuming a Saint-Venant constitutive model the total energy is given by :

$$H = \frac{1}{2} \int_\Omega \left(\rho A ||\boldsymbol{V}||^2 + \rho I W^2 + \boldsymbol{N}^\top \boldsymbol{C}_t \boldsymbol{N} + C_r M^2 \right) \mathrm{d}\Omega, \qquad \boldsymbol{C}_t = \mathrm{Diag} \begin{bmatrix} (EA)^{-1} \\ (kGA)^{-1} \end{bmatrix}, \quad C_r = (EI)^{-1}.$$

where E is Young's modulus, G the shear modulus and k the shear correction factor. The dual variables with respect to velocities and stress resultants are obtained by duality taking the derivative of the total energy (also called Hamiltonian)

$$\begin{aligned} \boldsymbol{\Pi}_V &:= \partial_{\boldsymbol{V}} H = \rho A \boldsymbol{V}, & \boldsymbol{\Gamma} &:= \partial_{\boldsymbol{N}} H = \boldsymbol{C}_t \boldsymbol{N}, \\ \Pi_W &:= \partial_W H = \rho I W, & K &:= \partial_M H = C_r M. \end{aligned}$$

where $\boldsymbol{\Pi}_V, \Pi_W$ are the linear and angular momenta, $\boldsymbol{\Gamma}$ the axial strain and K the curvature. The intrinsic formulation writes the dynamics in terms of velocities and stress resultants, leading to

$$\mathrm{Diag} \begin{bmatrix} \rho A \\ \rho I \\ \boldsymbol{C}_t \\ C_r \end{bmatrix} \partial_t \begin{pmatrix} \boldsymbol{V} \\ W \\ \boldsymbol{N} \\ M \end{pmatrix} = \begin{bmatrix} 0 & \boldsymbol{S}\boldsymbol{\Pi}_V & \boldsymbol{S}^\top K + \partial_s & 0 \\ \boldsymbol{\Pi}_V^\top \boldsymbol{S} & 0 & (\boldsymbol{\Gamma} + \boldsymbol{e}_1)^\top \boldsymbol{S} & \partial_s \\ \boldsymbol{S}^\top K + \partial_s & \boldsymbol{S}(\boldsymbol{\Gamma} + \boldsymbol{e}_1) & 0 & 0 \\ 0 & \partial_s & 0 & 0 \end{bmatrix} \begin{pmatrix} \boldsymbol{V} \\ W \\ \boldsymbol{N} \\ M \end{pmatrix}, \tag{2}$$

where $\boldsymbol{e}_1 = [1,0]^\top$. The Hamiltonian and more generally port-Hamiltonian structure of this model has been highlighted in [5, 6]. Further, the first two lines correspond to the local balance equations of momentum (1), here completely avoiding displacement-type quantities. If required these can be integrated from $\partial_t \boldsymbol{r} = \boldsymbol{\Lambda} \boldsymbol{V}$ and $\partial_t \theta = W$. The second two lines describe the stress-evolution in terms of the stress quantities in compliance form.

3 Discretization strategy

The discretization is explained in the linear case for simplicity as the nonlinearies are discretized by projection on a suitable finite element space. The simulations in Sec. 4 will be performed considering all nonlinear terms. In the process of a linearization all nonlinear terms can be dropped such that the linearized system reads :

$$\operatorname{Diag}\begin{bmatrix}\rho A\\ \rho I\\ \boldsymbol{C}_t\\ C_r\end{bmatrix}\partial_t\begin{pmatrix}\boldsymbol{V}\\ W\\ \boldsymbol{N}\\ M\end{pmatrix}=\begin{bmatrix}0 & 0 & \partial_s & 0\\ 0 & 0 & \boldsymbol{e}_1^\top \boldsymbol{S} & \partial_s\\ \partial_s & \boldsymbol{S}\boldsymbol{e}_1 & 0 & 0\\ 0 & \partial_s & 0 & 0\end{bmatrix}\begin{pmatrix}\boldsymbol{V}\\ W\\ \boldsymbol{N}\\ M\end{pmatrix}. \tag{3}$$

The weak form of the linear system (3) is given by :

$$\begin{aligned}
(\boldsymbol{\psi}_V, \rho A \partial_t \boldsymbol{V})_\Omega &= (\boldsymbol{\psi}_V, \partial_s \boldsymbol{N})_\Omega,\\
(\boldsymbol{\psi}_W, \rho I \partial_t W)_\Omega &= (\psi_W, \boldsymbol{e}_1^\top \boldsymbol{S}\boldsymbol{N})_\Omega + (\psi_W, \partial_s M)_\Omega,\\
(\boldsymbol{\psi}_N, \boldsymbol{C}_t \partial_t \boldsymbol{N})_\Omega &= (\boldsymbol{\psi}_N, \boldsymbol{S}\boldsymbol{e}_1 W)_\Omega + (\boldsymbol{\psi}_N, \partial_s \boldsymbol{V})_\Omega,\\
(\psi_M, C_r \partial_t M)_\Omega &= (\psi_M, \partial_s W)_\Omega,
\end{aligned} \tag{4}$$

where $(\cdot,\cdot)_\Omega$ is the L^2 inner product and $\psi_\square$ are appropriate test functions. Different integration by parts lead to different causalities in the final system. This happens at the discrete level but can be shown at the continuous level. If required, the discretization of displacement quantities can be obtained from a simple projection onto the same finite element spaces as the velocities.

3.1 The free-free case

This approach is in line with the common procedure in computational mechanics. If the first two lines are integrated by parts then one obtains :

$$\begin{aligned}
(\boldsymbol{\psi}_V, \rho A \partial_t \boldsymbol{V})_\Omega &= -(\partial_s \boldsymbol{\psi}_V, \boldsymbol{N})_\Omega + \langle \boldsymbol{\psi}_V, \boldsymbol{N}\rangle_{\partial\Omega},\\
(\boldsymbol{\psi}_W, \rho I \partial_t W)_\Omega &= (\boldsymbol{\psi}_W, \boldsymbol{e}_1^\top \boldsymbol{S}\boldsymbol{N})_\Omega - (\partial_s \boldsymbol{\psi}_W, M)_\Omega + \langle \boldsymbol{\psi}_W, M\rangle_{\partial\Omega},\\
(\boldsymbol{\psi}_N, \boldsymbol{C}_t \partial_t \boldsymbol{N})_\Omega &= (\boldsymbol{\psi}_N, \boldsymbol{S}\boldsymbol{e}_1 W)_\Omega + (\boldsymbol{\psi}_N, \partial_s \boldsymbol{V})_\Omega,\\
(\psi_M, C_r \partial_t M)_\Omega &= (\psi_M, \partial_s W)_\Omega,
\end{aligned}$$

where $\langle f, g\rangle_{\partial\Omega} = f(L,t)g(L,t) - f(0,t)g(0,t)$ for scalar fields and $\langle \boldsymbol{f}, \boldsymbol{g}\rangle_{\partial\Omega} = \boldsymbol{f}(L,t)\cdot\boldsymbol{g}(L,t) - \boldsymbol{f}(0,t)\cdot\boldsymbol{g}(0,t)$ for vector fields. Hat functions (linear continuous Galerkin CG_1) are used for the linear and angular velocity and piecewise constants are used for the axial and bending stress (discontinuous Galerkin DG_0)

$$\boldsymbol{V} \in [\mathrm{CG}_1]^2,\ W \in \mathrm{CG}_1, \qquad \boldsymbol{N} \in [\mathrm{DG}_0]^2,\ M \in \mathrm{DG}_0.$$

This choice makes some relationships between the variables exact [10] and it eliminates shear locking phenomena [7]. Indeed the relation $\partial_x \mathrm{CG}_1 = \mathrm{DG}_0$ is satisfied by these spaces, cf. Figs 1. Introducing the finite element approximation using a constant mesh size h and element number n the following ODE is obtained

$$\operatorname{Diag}\begin{bmatrix}\rho A \mathbf{M}_2\\ \rho I \mathbf{M}\\ h\boldsymbol{C}_t \otimes \mathbf{I}_n\\ C_r h \mathbf{I}_n\end{bmatrix}\frac{\mathrm{d}}{\mathrm{d}t}\begin{pmatrix}\mathbf{v}\\ \mathbf{w}\\ \mathbf{n}\\ \mathbf{m}\end{pmatrix}=\begin{bmatrix}0 & 0 & -\mathbf{D}_2^\top & 0\\ 0 & 0 & \mathbf{S} & -\mathbf{D}^\top\\ \mathbf{D}_2 & -\mathbf{S}^\top & 0 & 0\\ 0 & \mathbf{D} & 0 & 0\end{bmatrix}\begin{pmatrix}\mathbf{v}\\ \mathbf{w}\\ \mathbf{n}\\ \mathbf{m}\end{pmatrix}+\begin{bmatrix}\mathbf{T}_2^\top & 0\\ 0 & \mathbf{T}^\top\\ 0 & 0\\ 0 & 0\end{bmatrix}\begin{pmatrix}\mathbf{u}_N\\ \mathbf{u}_M\end{pmatrix}, \tag{5}$$

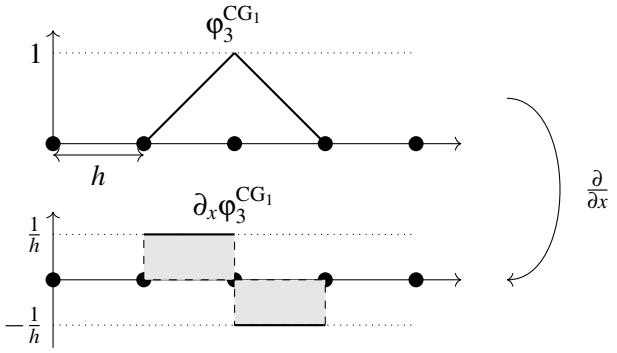

FIGURE 1 – Derivative of a Lagrange space CG_1, leading to a piecewise constant function.

The notation $\mathbf{A}_2$ indicates that the matrix $\mathbf{A}$ is repeated $i-$times on the diagonal of the resulting matrix and can be written using the Kronecker product as $\mathbf{A}_2 = \mathbf{I}_2 \otimes \mathbf{A}$. Furthermore, $\mathbf{v} \in \mathbb{R}^{2n+2}, \mathbf{w} \in \mathbb{R}^{n+1}, \mathbf{n} \in \mathbb{R}^{2n}$, $\mathbf{m} \in \mathbb{R}^n$ are vectors containing the finite element unknowns, $\mathbf{M} \in \mathbb{R}^{(n+1)\times(n+1)}$ is the mass matrix obtained when using Lagrange basis and $\mathbf{D} \in \mathbb{R}^{n\times(n+1)}$ is an approximation matrix of the spatial derivative operator, $\mathbf{S} \in \mathbb{R}^{(n+1)\times 2n}$ is the discretization of the cross product term and $\mathbf{T} \in \mathbb{R}^{2\times(n+1)}$ is a localization matrix that picks the degrees of freedom at the boundary. The input to the systems are the forces and bending moments at the extremities :

$$\mathbf{u}_N = \begin{pmatrix} -\boldsymbol{N}(0,t) \\ +\boldsymbol{N}(L,t) \end{pmatrix}, \qquad \mathbf{u}_M = \begin{pmatrix} -M(0,t) \\ +M(L,t) \end{pmatrix},$$

and we can write (5) more compactly :

$$\begin{aligned} \mathbf{M}_{FF}\dot{\mathbf{x}}_{FF} &= \mathbf{J}_{FF}\mathbf{x}_{FF} + \mathbf{B}_{FF}\mathbf{u}_{FF}, \\ \mathbf{y}_{FF} &= \mathbf{B}_{FF}^{\top}\mathbf{x}_{FF}. \end{aligned}$$

with $\mathbf{J}_{FF} = -\mathbf{J}_{FF}^{\top}$. The power conjugated outputs (the linear and angular velocities), have been added to interconnect systems with different boundary conditions. The resulting system can be represented via a block diagram as in Fig. 2. The dual formulation to the free-free one is the

FIGURE 2 – Block diagram for the free-free case

clamped-clamped one. Since this latter will not be used in the numerical examples, we omit it for the sake of brevity.

3.2 Pinned case

If the second and third lines of (4) are integrated by parts then one obtains :

$$\begin{aligned} &(\boldsymbol{\psi}_V, \rho A \partial_t \boldsymbol{V})_\Omega = (\boldsymbol{\psi}_V, \partial_s \boldsymbol{N})_\Omega, \\ &(\boldsymbol{\psi}_W, \rho I \partial_t W)_\Omega = (\boldsymbol{\psi}_W, \boldsymbol{e}_1^{\top}\boldsymbol{S}\boldsymbol{N})_\Omega - (\partial_s \boldsymbol{\psi}_W, M)_\Omega + \langle \boldsymbol{\psi}_W, M\rangle_{\partial\Omega}, \\ &(\boldsymbol{\psi}_n, \boldsymbol{C}_t \partial_t \boldsymbol{N})_\Omega = (\boldsymbol{\psi}_n, \boldsymbol{S}\boldsymbol{e}_1 W)_\Omega - (\partial_s \boldsymbol{\psi}_n, \boldsymbol{V})_\Omega + \langle \boldsymbol{\psi}_n, \boldsymbol{V}\rangle_{\partial\Omega}, \\ &(\psi_m, C_r \partial_t M)_\Omega = (\psi_m, \partial_s W)_\Omega. \end{aligned}$$

Piecewise constants are used for the linear velocity and bending moment, whereas hat functions are used for the angular velocity and axial stress resultant :

$$\boldsymbol{V} \in [\mathrm{DG}_0]^2,\ M \in \mathrm{DG}_0, \qquad W \in \mathrm{CG}_1,\ \boldsymbol{N} \in [\mathrm{CG}_1]^2.$$

such that we obtain after discretization :

$$\text{Diag}\begin{bmatrix}\rho A h\mathbf{I}_{2n}\\ \rho I\mathbf{M}\\ C_t\otimes\mathbf{M}\\ C_r h\mathbf{I}_n\end{bmatrix}\frac{\mathrm{d}}{\mathrm{d}t}\begin{pmatrix}\mathbf{v}\\ \mathbf{w}\\ \mathbf{n}\\ \mathbf{m}\end{pmatrix}=\begin{bmatrix}0 & 0 & \mathbf{D}_2 & 0\\ 0 & 0 & \mathbf{S} & -\mathbf{D}^\top\\ -\mathbf{D}_2^\top & -\mathbf{S}^\top & 0 & 0\\ 0 & \mathbf{D} & 0 & 0\end{bmatrix}\begin{pmatrix}\mathbf{v}\\ \mathbf{w}\\ \mathbf{n}\\ \mathbf{m}\end{pmatrix}+\begin{bmatrix}0 & 0\\ \mathbf{T}^\top & 0\\ 0 & \mathbf{T}_{n,2}^\top\\ 0 & 0\end{bmatrix}\begin{pmatrix}\mathbf{u}_M\\ \mathbf{u}_V\end{pmatrix},$$

where $\mathbf{T}_n$ is the normal trace matrix, taking values 1 or -1 for the right and left extremity. In a more compact form we can write

$$\begin{aligned}\mathbf{M}_{PP}\dot{\mathbf{x}}_{PP}&=\mathbf{J}_{PP}\mathbf{x}_{PP}+\mathbf{B}_{PP}\mathbf{u}_{PP},\\ \mathbf{y}_{PP}&=\mathbf{B}_{PP}^\top\mathbf{x}_{PP},\end{aligned}$$

and refer to Fig. 3 for an illustration of the causality.

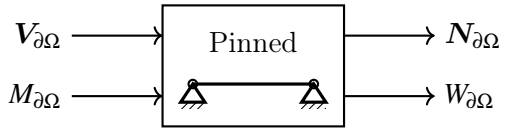

FIGURE 3 – Block diagram for the pinned-pinned case

3.3 Extension to the non linear case and time integration

The nonlinear terms in (2) do not require any special treatment at the numerical level (the nonlinearities do not involve any derivatives). Once a Galerkin finite element formulation is applied to the weak form of (2), a final system of the following form is obtained :

$$\begin{aligned}\mathbf{M}\dot{\mathbf{x}}&=\mathbf{J}_l\mathbf{x}+\mathbf{J}_{nl}(\mathbf{x})\mathbf{x}+\mathbf{B}\mathbf{u},\\ \mathbf{y}&=\mathbf{B}^\top\mathbf{x},\end{aligned}$$

where $\mathbf{J}_l=-\mathbf{J}_l^\top$ and $\mathbf{J}_{nl}=-\mathbf{J}_{nl}^\top$, which is linear in the state $\mathbf{x}$. Notice that the system exhibits a port-Hamiltonian structure and the Hamiltonian is quadratic in the state variable, meaning that $H=\frac{1}{2}\mathbf{x}^\top\mathbf{M}\mathbf{x}$. We now propose an implicit midpoint scheme as :

$$\begin{aligned}\mathbf{M}\frac{\mathbf{x}_{n+1}-\mathbf{x}_n}{\Delta t}&=\mathbf{J}_l\mathbf{x}_{n+1/2}+\mathbf{J}_{nl}(\mathbf{x}_{n+1/2})\mathbf{x}_{n+1/2}+\mathbf{B}\mathbf{u}_{n+1/2},\qquad \mathbf{x}_{n+1/2}:=\frac{\mathbf{x}_n+\mathbf{x}_{n+1}}{2},\\ \mathbf{y}_{n+1/2}&=\mathbf{B}^\top\mathbf{x}_{n+1/2}.\end{aligned}$$

The power balance equation for H is exactly preserved as :

$$\begin{aligned}\mathbf{x}_{n+1/2}^\top\mathbf{M}\frac{\mathbf{x}_{n+1}-\mathbf{x}_n}{\Delta t}&=\mathbf{x}_{n+1/2}^\top\left[\mathbf{J}_l\mathbf{x}_{n+1/2}+\mathbf{J}_{nl}(\mathbf{x}_{n+1/2})\mathbf{x}_{n+1/2}+\mathbf{B}\mathbf{u}_{n+1/2}\right]\\ &=\mathbf{x}_{n+1/2}^\top\mathbf{B}\mathbf{u}_{n+1/2},\qquad \text{By the skew-symmetry of } \mathbf{J}_l,\ \mathbf{J}_{nl}\\ &=\mathbf{y}_{n+1/2}^\top\mathbf{u}_{n+1/2}.\end{aligned}$$

The left hand side term becomes :

$$\begin{aligned}\mathbf{x}_{n+1/2}^\top\mathbf{M}\frac{\mathbf{x}_{n+1}-\mathbf{x}_n}{\Delta t}&=\left(\frac{\mathbf{x}_n+\mathbf{x}_{n+1}}{2}\right)^\top\mathbf{M}\frac{\mathbf{x}_{n+1}-\mathbf{x}_n}{\Delta t},\\ &=\frac{\mathbf{x}_{n+1}^\top\mathbf{M}\mathbf{x}_{n+1}-\mathbf{x}_n^\top\mathbf{M}\mathbf{x}_n}{2\Delta t},\\ &=\frac{H(\mathbf{x}_{n+1})-H(\mathbf{x}_n)}{\Delta t}.\end{aligned}$$

The following power balance is then obtained :

$$\frac{H(\mathbf{x}_{n+1})-H(\mathbf{x}_n)}{\Delta t}=\nabla H(\mathbf{x}_{n+1/2})^\top\left(\frac{\mathbf{x}_{n+1}-\mathbf{x}_n}{\Delta t}\right)=\mathbf{y}_{n+1/2}^\top\mathbf{u}_{n+1/2}.$$

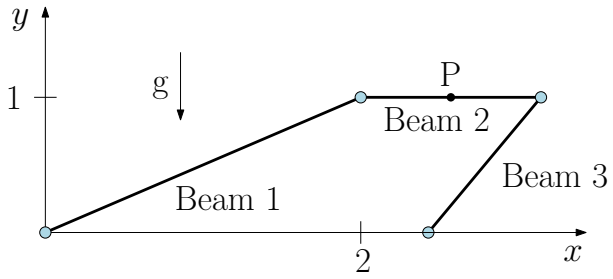

FIGURE 4 – Closed-loop kinematic chain

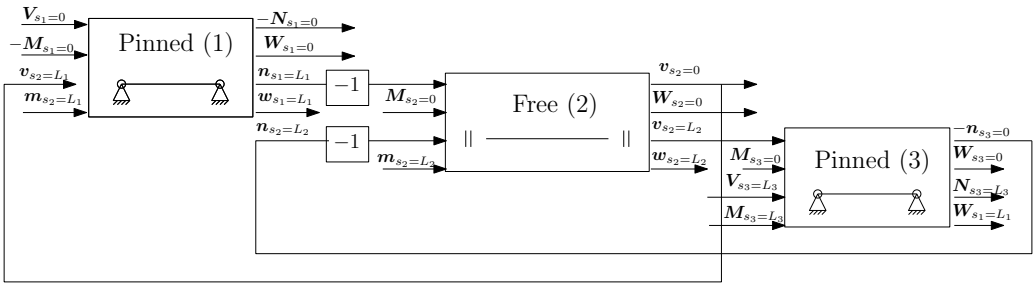

FIGURE 5 – Block diagram for the four bar mechanism

4 A closed loop kinematic mechanism

The proposed methodology makes it possible to represent closed loop kinematics without making use of algebraic multipliers. The system is subjected to gravity acting in the negative y-direction, which is incorporated into the proposed formulation by including distributed input forces with constant value $\boldsymbol{n}_{\text{ext}} = -g\rho A\boldsymbol{e}_2$. Beams 1 and 3 are connected to the ground through revolute support joints, cf. Fig. 4. To explain the interconnection algebraically, consider the dynamics of the pinned and free beam where the input to the left and right extremities are explicitly considered. Furthermore, as the bending moments are zero at the pins, the bending moment input is set to zero for all models meaning $\mathbf{u}_M = 0$.

$$\begin{aligned}
\mathbf{M}_{PP}\dot{\mathbf{x}}_{PP} &= \mathbf{J}_{PP}\mathbf{x}_{PP} + \mathbf{B}_{V,L}u_{V,L} + \mathbf{B}_{V,R}u_{V,R}, & \mathbf{M}_{FF}\dot{\mathbf{x}}_{FF} &= \mathbf{J}_{FF}\mathbf{x}_{FF} + \mathbf{B}_{N,L}u_{N,L} + \mathbf{B}_{N,R}u_{N,R},\\
y_{N,L} &= \mathbf{B}_{V,L}^{\top}\mathbf{x}_{PP}, & y_{V,L} &= \mathbf{B}_{N,L}^{\top}\mathbf{x}_{FF},\\
y_{N,R} &= \mathbf{B}_{V,R}^{\top}\mathbf{x}_{PP}, & y_{V,R} &= \mathbf{B}_{N,R}^{\top}\mathbf{x}_{FF}.
\end{aligned}$$

The feedback (or gyrator) interconnection is essentially Newton's third law :

$$\begin{aligned}
u_{V,R} &= +y_{V,L}, && \text{The velocity is the same on both sides,}\\
u_{N,L} &= -y_{N,R}, && \text{The forces are opposite.}
\end{aligned}$$

The interconnected system can be written as follows

$$\begin{bmatrix}\mathbf{M}_{PP} & 0\\ 0 & \mathbf{M}_{FF}\end{bmatrix}\begin{pmatrix}\dot{\mathbf{x}}_{PP}\\ \dot{\mathbf{x}}_{FF}\end{pmatrix} = \begin{bmatrix}\mathbf{J}_{PP} & +\mathbf{B}_{V,R}\mathbf{B}_{N,L}^{\top}\\ -\mathbf{B}_{N,L}\mathbf{B}_{V,R}^{\top} & \mathbf{J}_{FF}\end{bmatrix}\begin{pmatrix}\mathbf{x}_{PP}\\ \mathbf{x}_{FF}\end{pmatrix} + \begin{bmatrix}\mathbf{B}_{V,L} & 0\\ 0 & \mathbf{B}_{N,R}\end{bmatrix}\begin{pmatrix}\mathbf{u}_{V,L}\\ \mathbf{u}_{N,R}\end{pmatrix},$$
$$\begin{pmatrix}\mathbf{y}_{V,L}\\ \mathbf{y}_{N,R}\end{pmatrix} = \begin{bmatrix}\mathbf{B}_{V,L}^{\top} & 0\\ 0 & \mathbf{B}_{N,R}^{\top}\end{bmatrix}\begin{pmatrix}\mathbf{x}_{PP}\\ \mathbf{x}_{FF}\end{pmatrix}.$$

The interconnection corresponds to a feedback of two dynamical systems. An analogous interconnection is then performed between the resulting system and the pinned beam to obtain the structure. The corresponding block-diagram is shown in Fig. 5.

The analysis focuses on the motion of the center point P of the middle beam, whose initial position is given by $\boldsymbol{r}_{\mathsf{P}}(t=0) = (2.75, 1.5)$. The position vector has been obtained considering a finite element projection of the relation $\partial_t \boldsymbol{r} = \boldsymbol{\Lambda}\boldsymbol{V}$, leading to

$$(\boldsymbol{\psi}_r, \partial_t \boldsymbol{r})_\Omega = (\boldsymbol{\psi}_r, \boldsymbol{\Lambda}\boldsymbol{V})_\Omega, \qquad \text{forall } \boldsymbol{\psi}_r.$$

Δt	T	$N_{\text{elements}} = L/h$	L	ρ	A	I	E	ν
0.02	10	$\{10,6,6\}$	$\{\sqrt{5},1.5,\sqrt{2}\}$	2710	0.05^2	$0.05^4/12$	$2.1\cdot 10^{11}$	0.3

TABLE 1 – Parameters for the multibody system.

The finite element basis for the position is chosen to be the same as the velocity. For the free-free model, this corresponds to a Lagrange hat function $\boldsymbol{r} \in [\mathrm{CG}_1]^2$. The corresponding algebraic system reads

$$\mathbf{M}_2\dot{\mathbf{r}} = \mathbf{R}(\theta)\mathbf{v}.$$

The position of point P and the configurations of the system at different time instants are shown in Fig. 6 and coincide with the findings in [7]. Fig. 7 verifies the discrete-time energy-preservation of the proposed integration approach.

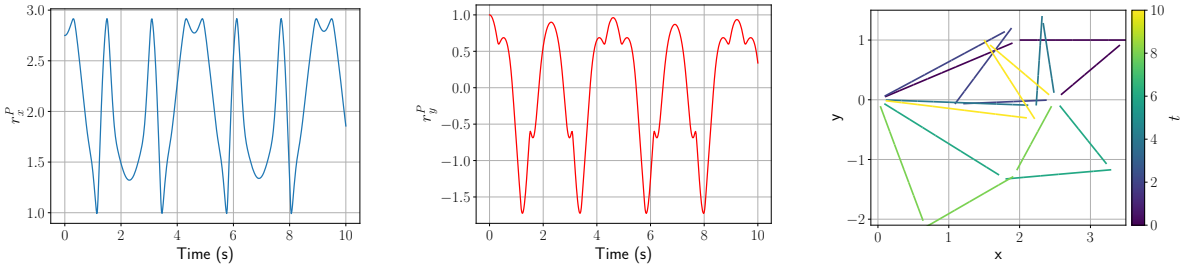

(a) $r_{\mathsf{P},x}(t)$ (b) $r_{\mathsf{P},y}(t)$ (c) Configurations

FIGURE 6 – Results for the closed loop multibody mechanism

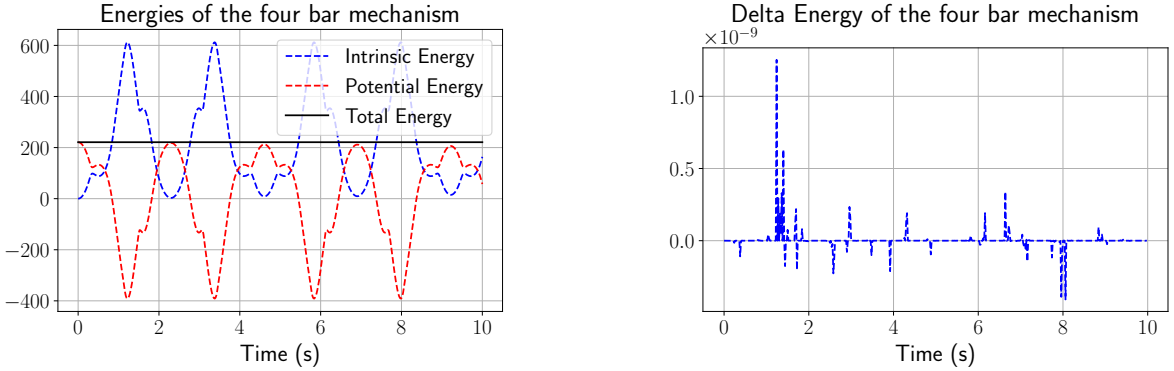

(a) (b)

FIGURE 7 – Intrinsic, i.e. $H = E_{\text{kin}} + E_{\text{def}}$, potential energy and total energy (a) and total energy increments (b).

5 Conclusion

In this paper, a structure-preserving discretization for multibody systems of geometrically exact beams has been proposed. The strategy relies on an intrinsic port-Hamiltonian beam model with different mixed finite element representations, that allow extracting different natural boundary conditions. The methodology is detailed for the pinned-pinned and free-free cases. Given the quadratic Hamiltonian structure, the implicit midpoint integrator allows preserving the energy and momentum exactly. This methodology provides the possibility of assembling some multibody systems without Lagrange multipliers. We have shown its application to a closed-loop kinematic chain.

Références

[1] Eric Reissner. On one-dimensional finite-strain beam theory : The plane problem. *Zeitschrift für angewandte Mathematik und Physik ZAMP*, 23(5) :795–804, 1972.

[2] J.C. Simo. A finite strain beam formulation. the three-dimensional dynamic problem. part i. *Computer Methods in Applied Mechanics and Engineering*, 49(1) :55–70, 1985.

[3] Dewey H. Hodges. Geometrically exact, intrinsic theory for dynamics of curved and twisted anisotropic beams. *AIAA Journal*, 41(6) :1131–1137, 2003.

[4] Charlotte Margot Rodriguez. *Control and stabilization of geometrically exact beams.* PhD thesis, Friedrich-Alexander-Universitaet Erlangen-Nuernberg (Germany), 2021.

[5] Rafael Palacios. Nonlinear normal modes in an intrinsic theory of anisotropic beams. *Journal of Sound and Vibration*, 330(8) :1772–1792, 2011.

[6] Marc Artola, Andrew Wynn, and Rafael Palacios. Modal-based nonlinear model predictive control for 3-d very flexible structures. *IEEE Transactions on Automatic Control*, 67(5) :2145–2160, 2021.

[7] Philipp L. Kinon, Peter Betsch, and Simon R. Eugster. Energy-momentum-consistent simulation of planar geometrically exact beams in a port-Hamiltonian framework. *Multibody System Dynamics*, Jun 2025.

[8] Pedram Khaneh Masjedi, Sajad Jangravi, and Alessandro Reali. Isogeometric collocation for locking-free large deflection analysis of geometrically exact beams with intrinsic formulation. *Computer Methods in Applied Mechanics and Engineering*, 446 :118282, 2025.

[9] Olivier Andre Bauchau. *Flexible multibody dynamics*, volume 176. Springer, 2011.

[10] Andrea Brugnoli, Denis Matignon, and Joseph Morlier. A linearly-implicit energy-momentum preserving scheme for geometrically nonlinear mechanics based on non-canonical Hamiltonian formulations. *Nonlinear Dynamics*, 113(20) :27539–27566, 2025.